The quantum spin-1/2 J_1–J_2 antiferromagnet on a stacked square lattice: a study of effective-field theory in a finite cluster

2010 J. Phys.: Condens. Matter 22 146004

(http://iopscience.iop.org/0953-8984/22/14/146004)

J. Phys.: Condens. Matter **22** (2010) 146004 (7pp) doi:10.1088/0953-8984/22/14/146004

The quantum spin-1/2 J_1–J_2 antiferromagnet on a stacked square lattice: a study of effective-field theory in a finite cluster

Wagner A Nunes[1], J Ricardo de Sousa[1,2], J Roberto Viana[1] and J Richter[3]

[1] Departamento de Física, Universidade Federal do Amazonas, 3000, Japiim, 69077-000, Manaus-AM, Brazil
[2] National Institute of Science and Technology for Complex Systems, Departamento de Física, 3000, Japiim, 69077-000, Manaus-AM, Brazil
[3] Institut für Theoretische Physik, Universität Magdeburg, PO Box 4120, 39016 Magdeburg, Germany

Received 19 September 2009, in final form 14 January 2010
Published 19 March 2010
Online at stacks.iop.org/JPhysCM/22/146004

Abstract
The ground state phase diagram of the quantum spin-1/2 Heisenberg antiferromagnet in the presence of nearest-neighbor (J_1) and next-nearest-neighbor (J_2) interactions (J_1–J_2 model) on a stacked square lattice, where we introduce an interlayer coupling through nearest-neighbor bonds of strength $J_\perp$, is studied within the framework of the differential operator technique. The Hamiltonian is solved by effective-field theory in a cluster with $N = 4$ spins (EFT-4). We obtain the sublattice magnetization m_A for the ordered phases: antiferromagnetic (AF) and collinear (CAF—collinear antiferromagnetic). We propose a functional for the free energy $\Psi_\mu(m_\mu)$ ($\mu = A, B$) to obtain the phase diagram in the λ–α plane, where $\lambda = J_\perp/J_1$ and $\alpha = J_2/J_1$. Depending on the values of λ and α, we found different ordered states (AF and CAF) and a disordered state (quantum paramagnetic (QP)). For an intermediate region $\alpha_{1c}(\lambda) < \alpha < \alpha_{2c}(\lambda)$ we observe a QP phase that disappears for λ below some critical value $\lambda_1 \simeq 0.67$. For $\alpha < \alpha_{1c}(\lambda)$ and $\alpha > \alpha_{2c}(\lambda)$, and below λ_1, we have the AF and CAF semi-classically ordered states, respectively. At $\alpha = \alpha_{1c}(\lambda)$ a second-order transition between the AF and QP states occurs and at $\alpha = \alpha_{2c}(\lambda)$ a first-order transition between the AF and CAF phases takes place. The boundaries between these ordered phases merge at the critical end point CEP $\equiv (\lambda_1, \alpha_c)$, where $\alpha_c \simeq 0.56$. Above this CEP there is again a direct first-order transition between the AF and CAF phases, with a behavior described by the point α_c independent of $\lambda \geqslant \lambda_1$.

1. Introduction

Recently, studies of low-dimensional spin quantum systems have been of great interest because enhanced quantum fluctuations lead to unusual ground states and unusual low-temperature properties. At null temperature, we have an absence of thermal fluctuations and the phase transitions between the ground state are driven purely by the interplay of quantum mechanical fluctuations and competition between interactions [1].

One of the models most studied in the past is that of a spin-1/2 Heisenberg antiferromagnet [2]. The quantum Heisenberg antiferromagnet is a canonical model to describe quantum phase transitions. In particular, the two-dimensional (2D) quantum spin-1/2 Heisenberg model with competing nearest-neighbor (nn) and next-nearest-neighbor (nnn) antiferromagnet exchange interactions (i.e. *frustration*) on a square lattice (J_1–J_2 model) has been exhaustively studied by several methods [3–16], where the critical properties are relatively well known. In the absence of the nnn (next-nearest-neighbor) interactions (i.e. $J_2 = 0$), the system is not frustrated and the ground state possesses antiferromagnetic (AF) long-range order (LRO) with wavevector $\mathbf{Q} = (\pi, \pi)$. The presence of the nnn interactions is expected to induce strong frustration to

break the AF order, and a quantum paramagnetic (QP) phase between α_{1c} and α_{2c} ($\alpha = J_2/J_1$). For $\alpha > \alpha_{2c}$ we have two degenerate collinear states with wavevectors $\mathbf{Q} = (\pi, 0)$ and $(0, \pi)$ that are characterized by a parallel spin orientation of nearest neighbors in the vertical (or horizontal) direction and an antiparallel spin orientation of nearest neighbors in the horizontal (or vertical) direction and therefore exhibit Néel order within the initial sublattice A and B. The recent syntheses of magnetic materials such as Li_2VOSiO_4 and Li_2VOGeO_4 are well described by the J_1–J_2 model [17, 18] with $\alpha \simeq 1$ and have stimulated further interest in this quantum frustrated model. These two isostructural compounds are characterized by a layered structure containing V^{4+} ($S = 1/2$) ions. The structures of the V^{4+} layer suggest that the superexchange is similar with a small interlayer coupling $J_\perp = \lambda J_1$, where $\lambda \simeq 10^{-2}$. In general, an interlayer coupling $J_\perp$ may be relevant in real materials, it may have a crucial influence of the ground state magnetic ordering.

The nature of the transition between the AF and QP phases as well as the properties of the QP state as still under debate. Candidates examined for the QP phase are: a resonating-valence-bond (RVB) state [8], a plaquette state [20, 21], a dimer state [7], and a state with both dimer and plaquette structures [22]. Whether the QP phase is a singlet state with gapped excitations to the first triplet state [15] has also been investigated.

The critical properties of frustrated spin models strongly depend on the dimensionality (d), Hamiltonian symmetry (n) and spin (S). In particular, for the case of the 2d classical ($S \to \infty$) J_1–J_2 Heisenberg ($n = 3$) model there is a consensus regarding the non-existence of the QP state, with a first-order transition at $\alpha_c = 1/2$ that separates the AF and collinear phases. The Ising ($n = 1$) limit also present a direct first-order transition [23] at $\alpha_c = 1/2$. Quantum fluctuations can modify drastically the ground state behavior, inducing, for example, the QP state in the quantum spin-1/2 J_1–J_2 Heisenberg model on a square lattice. For the one-dimensional (1d) case, this model with spin $S = 1/2$ does not have an AF ordered ground state, but exhibits a transition from a critical state to a dimer state at $\alpha_c^q = 0.241$ critical point [24]. Although in three dimensions magnetic long-range order is more likely, a QP state may also be observed for frustrated 3d systems, e.g. for the Heisenberg antiferromagnet on the pyrochlore lattice [25]. The quantum spin-1/2 Heisenberg model on the body-centered cubic (bcc) [26] and simple cubic (sc) [27] lattices has been studied, and it was shown that this 3d quantum spin-1/2 J_1–J_2 model does not have a quantum disordered QP phase, rather it exhibits a direct zero-temperature first-order phase transition at α_c^q ($\alpha_c^q \simeq 0.70$ and 0.21 for the bcc and sc lattices, respectively) from the two-sublattice Néel phase to the so-called lamellar collinear state (sequences of up and down planes) driven by frustration J_2. The critical behavior of the square lattice version of the quantum spin-1/2 J_1–J_2 Heisenberg model has been studied for many years, but very little has been done in the 3d case.

From the experimental viewpoint, to explore the ground state phase diagram of frustrated compounds described by the J_1–J_2 model, the high to the low α regime can be investigated continuously by applying high pressure (P), which modifies the bonding lengths and angles. Recently, x-ray diffraction measurements [28] on the Li_2VOSiO_4 compound have shown that the ratio α decreases by about 40% when the pressure increases from 0 to 7.6 GPa.

The outline of the paper is as follows. In section 2, the model is presented and the formalism developed in section 3. In section 4, the results of the ground state phase diagram in the λ–α plane and the behavior of the order parameters in the AF and CAF phases are discussed. Finally, in section 5 we present a short conclusion.

2. The model

In this work, we consider the influence of such an interlayer coupling on the quantum spin-1/2 J_1–J_2 model on a simple cubic lattice, which is described by following Hamiltonian:

$$\mathcal{H} = \sum_n \left(J_1 \sum_{\langle i,j \rangle} \boldsymbol{\sigma}_{in} \cdot \boldsymbol{\sigma}_{jn} + J_2 \sum_{\langle\langle i,l \rangle\rangle} \boldsymbol{\sigma}_{in} \cdot \boldsymbol{\sigma}_{ln} \right) + J_\perp \sum_{i,n} \boldsymbol{\sigma}_{in} \cdot \boldsymbol{\sigma}_{in+1} \tag{1}$$

where $\boldsymbol{\sigma}_{in} = (\sigma_{in}^x, \sigma_{in}^y, \sigma_{in}^z)$ are the spin-1/2 Pauli operators at site i in the nth-layer on the simple cubic lattice. The first and second sums run over the nearest-neighbor (nn) and next-nearest-neighbor (nnn) spin pairs, respectively, J_1 ($J_2 = \alpha J_1$) is the nn (nnn) coupling and $J_\perp$ ($=\lambda J_1$) the interlayer coupling. In the two-dimensional limit ($\lambda = 0$), in the ground state phase diagram, the QP state is present, while in the isotropic 3d case ($\lambda = 1$) one may expect that this quantum disordered state is not observed. The main motivation of this work is to discuss the competition between the interlayer λ and frustration α parameters and to investigate their influence on the QP state. Here we consider the case of antiferromagnetic (AF) nn interactions that correspond to $J_1(J_\perp) > 0$.

The theoretical treatment of the frustrated quantum antiferromagnetism is far from being trivial. Many of the standard many-body methods, such as quantum Monte Carlo techniques, may fail or become computationally infeasible to implement if frustration is present due to the minus-sign problem. Hence, there is considerable interest in any method that can deal with frustrated spin systems. Recently [29], the model (1) has been studied for antiferromagnetic J_1 and $J_\perp$ by using the coupled-cluster (CCM) and rotation-invariant Green's function (RGM) methods. It was found, that for a characteristic value $\lambda_1 \simeq 0.31(0.19)$ the quantum paramagnetic phase (i.e. the QP state) disappears using the RGM (CCM) approach. This considerable difference in that value for λ_1 further motivates us to study this issue by alternative methods. In this paper we will use the effective-field theory (EFT) in a finite cluster to treat the model (1) and obtain the phase diagram at $T = 0$ (ground state). This method have been applied successfully to study a large variety of problems, in particular quantum models in arbitrary dimensions [30] and it is able to study frustrated models [16, 23, 27, 31, 32].

3. Effective-field theory

The starting point for the EFT calculation is to choose a finite cluster and obtain an average of spin operators by using the Callen and Suzuki generalized relation (for more details, see [30]). The EFT provides a hierarchy of approximations to obtain thermodynamic properties of magnetic models. One can continue this series of approximations to consider larger and larger clusters and as a consequence, better results are obtained. The exact solution would be obtained by considering an infinite cluster. However, by using relatively small clusters that contain the topology of the lattice, one can obtain a reasonable description of the thermodynamic properties. The model (1) in two ($\lambda = 0$) [16] and three ($\lambda = 1$) [27] dimensions was recently treated by EFT in a cluster with two spins (EFT-2), where the phase diagram at $T = 0$ and finite temperature was obtained. In this limit of zero interlayer parameter λ we have the presence of the QP phase, while in the three-dimensional limit the QP states have not been observed. For quantum spin systems, an appropriate choice for the ground state of the ordered phase is often a classical spin state.

To treat the phase diagram of the model (1), firstly the order parameters (magnetization of sublattice $m_{\rm A}$) of the AF and CAF ordered phases are calculated. As a starting point for this calculation ($m_{\rm A}$), we use the following expression for the average of a general function involving spin operator components $\mathcal{O}(\{n\})$

$$\langle \mathcal{O}(\{n\})\rangle = \left\langle \frac{{\rm Tr}_{\{n\}}\{\mathcal{O}(\{n\}){\rm e}^{-\beta\mathcal{H}_{\{n\}}}\}}{{\rm Tr}_{\{n\}}\{{\rm e}^{-\beta\mathcal{H}_{\{n\}}}\}}\right\rangle, \tag{2}$$

where the partial trace ${\rm Tr}_{\{n\}}\{\cdots\}$ is taken over the set $\{n\}$ of spin variables (finite cluster) specified by the multisite spin Hamiltonian $\mathcal{H}_{\{n\}}$ and $\langle\cdots\rangle$ indicates the usual canonical thermal average. The interactions within the cluster are treated exactly and the effect of the remaining lattice spins is treated by a given approximation (EFT).

In order to study the Hamiltonian (1), we use the four-site cluster approximation given by (see figure 1)

$$\begin{aligned}\mathcal{H}_4 &= J_1(\boldsymbol{\sigma}_a\cdot\boldsymbol{\sigma}_b + \boldsymbol{\sigma}_b\cdot\boldsymbol{\sigma}_{\rm c} + \boldsymbol{\sigma}_{\rm c}\cdot\boldsymbol{\sigma}_d + \boldsymbol{\sigma}_d\cdot\boldsymbol{\sigma}_a)\\ &\quad + \alpha J_1(\boldsymbol{\sigma}_a\cdot\boldsymbol{\sigma}_{\rm c} + \boldsymbol{\sigma}_b\cdot\boldsymbol{\sigma}_d) + \Delta\mathcal{H}_{o4},\end{aligned} \tag{3}$$

with

$$\Delta\mathcal{H}_{o4} = \sigma_a^z C_1 + \sigma_b^z C_2 + \sigma_{\rm c}^z C_3 + \sigma_d^z C_4, \tag{4}$$

$$C_1 = J_1(\sigma_1^z+\sigma_2^z)+\lambda J_1(\sigma_6^z+\sigma_{11}^z)+\alpha J_1(\sigma_3^z+\sigma_4^z+\sigma_5^z), \tag{5}$$

$$C_2 = J_1(\sigma_5^z+\sigma_{16}^z)+\lambda J_1(\sigma_{10}^z+\sigma_{15}^z)+\alpha J_1(\sigma_1^z+\sigma_{17}^z+\sigma_{18}^z), \tag{6}$$

$$C_3 = J_1(\sigma_{18}^z+\sigma_{22}^z)+\lambda J_1(\sigma_{20}^z+\sigma_{24}^z)+\alpha J_1(\sigma_{16}^z+\sigma_{25}^z+\sigma_{26}^z), \tag{7}$$

and

$$C_4 = J_1(\sigma_4^z+\sigma_{25}^z)+\lambda J_1(\sigma_9^z+\sigma_{14}^z)+\alpha J_1(\sigma_2^z+\sigma_{22}^z+\sigma_{31}^z), \tag{8}$$

where $\alpha = J_2/J_1$ and $\lambda = J_\perp/J_1$.

Substituting equation (3) in (2), we obtain the magnetization per spin in sublattice A by

$$m_{\rm A} = \langle\sigma_a^z\rangle = \left\langle -\frac{\partial \ln \mathcal{Z}_4(\mathbf{C})}{\partial\beta C_1}\right\rangle, \tag{9}$$

with the partition function

$$Z_4(\mathbf{C}) = {\rm Tr}_{\{\boldsymbol{\sigma}\}}\{{\rm e}^{-\beta\mathcal{H}_4}\}, \tag{10}$$

where $\mathbf{C} = (C_1, C_2, C_3, C_4)$ and $\{\boldsymbol{\sigma}\} = \{\boldsymbol{\sigma}_a, \boldsymbol{\sigma}_b, \boldsymbol{\sigma}_{\rm c}, \boldsymbol{\sigma}_d\}$.

We have also treated the model (1) by using a finite cluster with $N = 2$ spins (EFT-2), which was previously developed in [16, 27] to study the two- ($\lambda = 0$) and three- ($\lambda = 1$) dimensional limits. On the other hand, using EFT-2 we obtain not the phase diagram in the λ–α plane for all values of interlayer parameter (λ), only the particular limits ($\lambda = 0, 1$). Therefore, we extend our calculations of EFT for a cluster with $N = 4$ spins.

Using the identity $\exp(\mathbf{a}\cdot\mathbf{D})f(\mathbf{x}) = f(\mathbf{x}+\mathbf{a})$, where $\mathbf{D} = (D_1, D_2, D_3, D_4)$ and $\mathbf{a} = (a_1, a_2, a_3, a_4)$ are four-dimensional differential operator and vector, respectively, $D_\mu = \frac{\partial}{\partial x_\mu}$, the equation (9) can be rewritten as

$$\begin{aligned}m_{\rm A} = \langle &{\rm e}^{-K_1(D_1+\alpha D_2)\sigma_1^z}\cdot{\rm e}^{-K_1(D_1+\alpha D_4)\sigma_2^z}\cdot{\rm e}^{-K_1(D_2+\alpha D_1)\sigma_5^z}\\ &\cdot{\rm e}^{-K_1(D_2+\alpha D_3)\sigma_{16}^z}\cdot{\rm e}^{-K_1(D_3+\alpha D_2)\sigma_{18}^z}\cdot{\rm e}^{-K_1(D_3+\alpha D_4)\sigma_{22}^z}\\ &\cdot{\rm e}^{-K_1(D_4+\alpha D_1)\sigma_4^z}\cdot{\rm e}^{-K_1(D_4+\alpha D_3)\sigma_{25}^z}\\ &\cdot{\rm e}^{-\lambda K_1[(\sigma_6^z+\sigma_9^z)D_1+(\sigma_{10}^z+\sigma_{11}^z)D_2+(\sigma_{14}^z+\sigma_{15}^z)D_3+(\sigma_{20}^z+\sigma_{24}^z)D_4]}\\ &\cdot{\rm e}^{-\alpha K_1(\sigma_3^z D_1+\sigma_{17}^z D_2+\sigma_{26}^z D_3+\sigma_{31}^z D_4)}\rangle g(\mathbf{x})|_{\mathbf{x}=0},\end{aligned} \tag{11}$$

with

$$g(\mathbf{x}) = -\frac{\partial \ln \mathcal{Z}_4(\mathbf{x})}{\partial x_1}, \tag{12}$$

$$Z_4(\mathbf{x}) = {\rm Tr}_{\{\boldsymbol{\sigma}\}}\{{\rm e}^{-\mathcal{A}(\mathbf{x})}\}, \tag{13}$$

and

$$\begin{aligned}\mathcal{A}(\mathbf{x}) &= K_1(\boldsymbol{\sigma}_a\cdot\boldsymbol{\sigma}_b + \boldsymbol{\sigma}_b\cdot\boldsymbol{\sigma}_{\rm c} + \boldsymbol{\sigma}_{\rm c}\cdot\boldsymbol{\sigma}_d + \boldsymbol{\sigma}_d\cdot\boldsymbol{\sigma}_a)\\ &\quad + \alpha K_1(\boldsymbol{\sigma}_a\cdot\boldsymbol{\sigma}_{\rm c} + \boldsymbol{\sigma}_b\cdot\boldsymbol{\sigma}_d) + \sigma_a^z x_1 + \sigma_b^z x_2\\ &\quad + \sigma_{\rm c}^z x_3 + \sigma_d^z x_4,\end{aligned} \tag{14}$$

where $K_1 = \beta J_1$.

The operator (14) can be written in matrix form, where we use the basis of the $\{\sigma_a^z, \sigma_b^z, \sigma_{\rm c}^z, \sigma_d^z\}$ components for diagonalization, resulting in a 16×16 matrix. The matrix is diagonalized numerically and them the function $g(\mathbf{x})$ is obtained for a given value of reduced temperature $t = 1/K_1$, and fixed α and λ parameters.

Now using the van der Waerden identity for the σ_i^z component Pauli spin operator, i.e. $\exp(\lambda\sigma_i^z) = \cosh(\lambda) + \sigma_i^z\sinh(\lambda)$, equation (11) can be exactly written in terms of multiple spin correlation functions occurring on the right-hand side. However, it is clear that if we try to treat exactly all boundary spin–spin correlation functions, the problem becomes unmanageable. The simplest and most frequently used approximation (denoted by EFT-4) is to decouple them according to

$$\langle\sigma_i^z\cdot\sigma_j^z\cdots\sigma_l^z\rangle \simeq \langle\sigma_i^z\rangle\cdot\langle\sigma_j^z\rangle\cdots\langle\sigma_l^z\rangle \qquad (i\neq j\neq\cdots\neq l), \tag{15}$$

which means that the nearest and next-nearest neighbors of site i are assumed to be completely independent of each other. It should be noted here that the approximation (15) is quite superior to the standard mean-field theory (MFT), since within the present framework (EFT) the kinematics relations is taken exactly (i.e. $(\sigma_i^z)^2 = 1$) into account through the van der

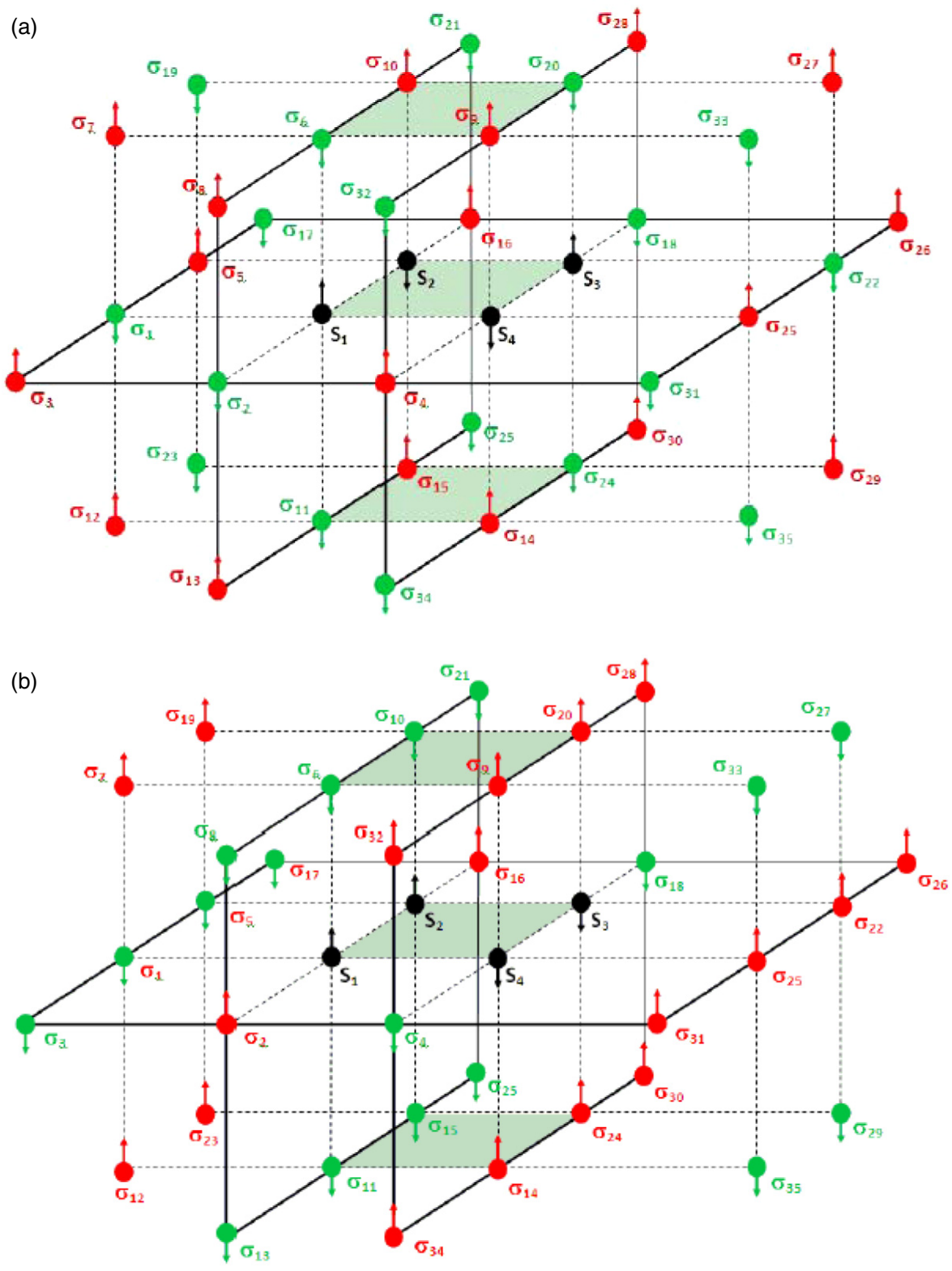

Figure 1. Ground state for a four-spin cluster in the AF (a) and CAF (b) phase structures. (This figure is in colour only in the electronic version)

Waerden identity, and, as a consequence, it neglects only correlations between different spin variables, while in the usual MFT all the self- and multi-spin correlations are neglected.

To obtain the equation of state in the AF phase (see figure 1(a)), we use the boundary conditions: (i) $\langle \sigma_i^z \rangle = -m_{\rm AF}$ for $i = 1, 2, 6, 11, 17, 18, 20, 22, 24$ and 31; (ii) $\langle \sigma_j^z \rangle = m_{\rm AF}$

for $j = 3, 4, 5, 9, 10, 14, 15, 16, 25$ and 26, which are given by

$$m_{\rm AF} = \Lambda_{\rm AF}(m_{\rm AF}, t, \alpha, \lambda) = \sum_{r=0}^{9} A_{2r+1}^{\rm AF}(t, \alpha, \lambda) m_{\rm AF}^{2r+1}, \quad (16)$$

where the coefficients $A_{2r+1}^{\rm AF}(t, \alpha, \lambda)$ are determined numerically by applying the identity $\exp(\mathbf{a}\cdot\mathbf{D})\, f(\mathbf{x}) = f(\mathbf{x}+\mathbf{a})$, and the final expressions are too lengthy and will be omitted.

On the other hand, the equation of state in the CAF phase (see figure 1(b)) is given by

$$m_{\rm CAF} = \Lambda_{\rm CAF}(m_{\rm CAF}, t, \alpha, \lambda) = \sum_{r=0}^{9} A_{2r+1}^{\rm CAF}(t, \alpha, \lambda) m_{\rm CAF}^{2r+1}, \quad (17)$$

where we have used the boundary conditions: (i) $\langle \sigma_i^z \rangle = -m_{\rm CAF}$ for $i = 1, 3, 4, 5, 6, 10, 11, 15, 17$ and 18; (ii) $\langle \sigma_j^z \rangle = m_{\rm CAF}$ for $j = 2, 9, 14, 16, 20, 22, 24, 25, 26$ and 31 to obtain equation (17).

Depending of the values of the parameters α and λ we observe first- and second-order transitions. We note that it is not possible to calculate the first-order transition line on the basis only of the equations of state (16) and (17). To solve this problem one needs to calculate the free energy for each state (AF, CAF and QP). Assuming that these equations of state are obtained by the minimization of a given energy functional like $\Psi_\mu(m_\mu)$ (i.e. $\frac{{\rm d}\Psi_\mu(m_\mu)}{{\rm d}m_\mu} = 0$ for $\mu =$ AF, CAF), after integration we obtain

$$\Psi_\mu(m_\mu) = \Delta_1(T, \alpha, \lambda) + \Delta_2(T, \alpha, \lambda) \times \left[1 - \sum_{r=0}^{9} \frac{A_{2r+1}^{\mu}(t, \alpha, \lambda)}{r+1} m_\mu^{2r}\right] \frac{m_\mu^2}{2}, \quad (18)$$

where $\Delta_1(T, \alpha, \lambda)$ and $\Delta_2(T, \alpha, \lambda)$ are arbitrary functions which turn out to be irrelevant when searching the second- and first-order transitions.

From equation (18), we obtain the point of intersection (Maxwell construction) between the free energy in the $\mu =$ AF, CAF ordered and QP ($m = 0$) disordered phases. This is given by

$$\sum_{r=0}^{9} \frac{A_{2r+1}^{\mu}(t, \alpha, \lambda)}{r+1} m_\mu^{2r} = 1. \quad (19)$$

In the case of the quantum phase transition between the two ordered phases (AF and CAF), using Maxwell construction we obtain

$$\sum_{r=0}^{9} \frac{A_{2r+1}^{\rm AF}(t, \alpha, \lambda)}{r+1} m_{\rm AF}^{2r+2} - m_{\rm AF}^2 = \sum_{r=0}^{9} \frac{A_{2r+1}^{\rm CAF}(t, \alpha, \lambda)}{r+1} m_{\rm CAF}^{2r+2} - m_{\rm CAF}^2. \quad (20)$$

4. Results: ground state

Solving the equation of state (16) at null temperature ($T = 0$), we observe that the order parameter $m_{\rm AF}(\alpha)$ in the AF phase falls smoothly to zero when the frustration parameter (α) increases from zero to $\alpha_{1c}(\lambda)$ when $\lambda < \lambda_1 \simeq 0.67$,

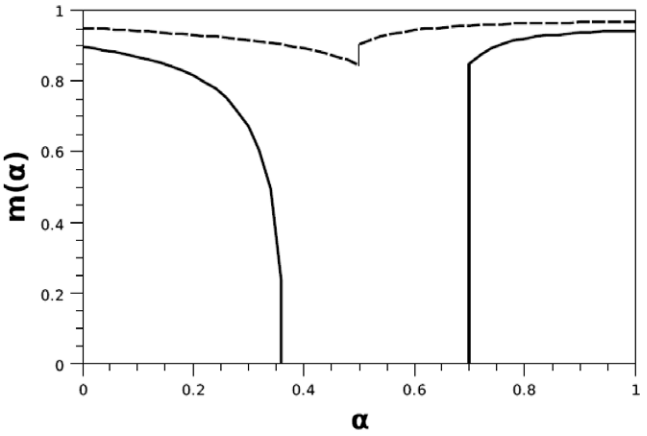

Figure 2. Frustration parameter dependence of the staggered magnetization in the AF and CAF phases for $\lambda = 0.2$ (solid curves) and $\lambda = 0.8$ (dashed curves) for the quantum spin-1/2 J_1–J_2 model on a stacked square lattice.

characterizing a second-order phase transition. On the other hand, for $\lambda < \lambda_1$ and $\alpha > \alpha_{2c}(\lambda)$ the staggered magnetization $m_{\rm CAF}(\alpha)$ in the CAF phase, equation (17), includes an unstable solution in addition to the stable solution. Using Maxwell construction, which corresponds then to that point in the phase diagram where the free energy between the QP and CAF phases are equal, we found, by simultaneously solving equations (17) and (19), the first-order transition point by using the discontinuity of the staggered magnetization $m_{\rm CAF}^*(\alpha)$ at $\alpha_{2c}^*(\lambda)$.

To illustrate the nature of the phase transition, we have shown in figure 2 the behavior of the staggered magnetization (order parameter) as a function of the frustration parameter (α) for $\lambda = 0.2$ ($<\lambda_1$) and $\lambda = 0.8$ ($>\lambda_1$), obtained numerically from equations (16) and (17) for both AF and CAF phases, respectively. From curves such as those shown in figure 2 we see that for $\lambda = 0.2$ (solid curves) there exists an intermediate region between the critical point $\alpha = \alpha_{1c}(\lambda)$ at which $m_{\rm AF}(\alpha) \to 0$ for the AF phase, characterizing a second-order transition, and the point $\alpha = \alpha_{2c}^*(\lambda)$ at which the order parameter presents a discontinuity for the CAF phase, characterizing a first-order transition. For $\lambda = 0.8$ (dashed curves), the order parameter of the AF phase decreases monotonically with increase of the frustration parameter from $\approx$0.875 for $\alpha = 0$ to $\approx$0.850 for $\alpha = \alpha_{2c}^*(\lambda) \simeq 0.56$. In the CAF phase $m_{\rm CAF}(\alpha)$ decreases from $\approx$0.890 for $\alpha = 1.0$ to $\approx$0.874 for $\alpha = \alpha_{2c}^*(\lambda) \simeq 0.56$, characterizing a direct first-order transition between the magnetically ordered AF and CAF phases located at the crossing point. This is similar to the three-dimensional J_1–J_2 model [26, 27], where we have a quantum point at $\alpha = \alpha_{2c}^*(\lambda) \simeq 0.56$. The disordered QP region disappears completely and we obtain two ordered phases: AF and CAF.

The ground state ($T = 0$) phase diagram of the anisotropic 3d quantum spin-1/2 J_1–J_2 Heisenberg model is shown in figure 3. It is dependent on the values of α and λ. We observe three phases, namely: AF (antiferromagnetic, see figure 1(a)), CAF (collinear antiferromagnetic, see figure 1(b))

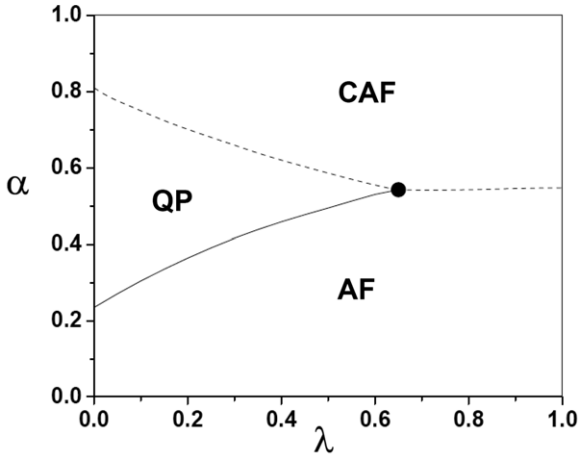

Figure 3. Ground state phase diagram in the λ–α plane for the quantum spin-1/2 J_1–J_2 model on a stacked square lattice. The dashed and solid lines correspond to the first- and second-order transitions, respectively. The black point represents the critical end point CEP. The notations indicated by AF, CAF and QP correspond the antiferromagnetic, collinear antiferromagnetic and quantum paramagnetic phases, respectively.

and QP (quantum paramagnetic). The AF and QP phases are separated by a second-order transition line $\alpha_{1c}(\lambda)$, while the QP and CAF phases are separate by a first-order transition line $\alpha_{2c}(\lambda)$. The presence of the interlayer parameter λ has the general effect to suppress the QP phase. The QP region decreases gradually with the increase of the parameter λ, and it disappears completely at the critical end point CEP $\equiv (\lambda_1, \alpha_1)$ where the boundaries between these phases merge. Above this CEP, i.e. for $\lambda > \lambda_1$, there is a direct first-order phase transition between the AF and CAF, with a transition point $\alpha_1 \simeq 0.56$ independent of $\lambda \geqslant \lambda_1$, in accordance with the results of [29]. To find the transition point $\alpha_{2c}(\lambda)$, we simultaneously solve the three transcendental expressions given by equations (16), (17) and (20). Such a direct first-order transition was also observed for the classical J_1–J_2 model and also for the quantum J_1–J_2 model on the body-centered cubic [26] and the simple cubic [27] lattices.

5. Conclusions

To summarize, it has been confirmed in previous work [14, 16] that exchange anisotropy reduces the quantum fluctuations and leads to a shrinking of the QP region of the J_1–J_2 model. In the present work, the quantum fluctuations in the J_1–J_2 Heisenberg model are tuned by an nn interlayer coupling of strength $J_\perp$. Again the reduction of quantum fluctuations leads to a shrinking of the QP region. We can compare our results obtained by EFT with available results obtained by the CCM and RGM approaches [29]. In [29] it was found that the QP phase disappears for $\lambda_1 \simeq 0.19$ (0.31) obtained by the CCM (RGM) approach. These results are in qualitative agreement with $\lambda_1 \simeq 0.76$ found in the present paper. However, the effective-field theory in clusters with four spins (EFT-4) seems to overestimate the value of λ_1.

We have firstly treated the model (1) by using a finite cluster with $N = 2$ spins (EFT-2), and the results have not been satisfactory, where we obtain not the phase diagram in the λ–α plane for all values of interlayer parameter (λ), only the $\lambda = 0$ and 1 particular limits. The EFT-2 was previously developed to study the two-($\lambda = 0$) [16] and three- ($\lambda = 1$) [27] dimensional J_1–J_2 model. Therefore, in this paper we have extended our calculations of EFT in clusters with $N = 4$ spins to study the phase diagram of the anisotropic J_1–J_2 model for all intervals of $\lambda \in [0, 1]$. The QP phase found earlier for $\lambda = 0$ in [16] for a cluster with $N = 2$ spins (EFT-2) has also has been found in the present paper, see figure 3. For a simple cubic lattice ($\lambda = 1$) we have a direct first-order transition between the AF and CAF phases, as observed recently by Viana *et al* [27] by using EFT-2.

Acknowledgments

This work was partially supported by CNPq and FAPEAM (Brazilian agencies).

References

[1] Sachdev S 1999 *Quantum Phase Transitions* (Cambridge: Cambridge University Press)
[2] Manousakis E 1991 *Rev. Mod. Phys.* **63** 1
[3] Chandra P and Doucot B 1988 *Phys. Rev.* B **38** 9335
[4] Ioffe L B and Larkin A I 1988 *Mod. Phys.* B **2** 203
[5] Richter J 1993 *Phys. Rev.* B **47** 5794
[6] Ivanov N B and Richter J 1994 *J. Phys.: Condens. Matter* **6** 3785
Richter J, Ivanov N B and Retzlaff K 1994 *Europhys. Lett.* **25** 545
[7] Singh R R P, Weihong Z, Hamer C J and Oitmaa J 1999 *Phys. Rev.* B **60** 7278
[8] Capriotti L, Fubini A, Roscilde T and Tognetti V 2004 *Phys. Rev. Lett.* **92** 157202
[9] Weber C, Becca F and Mila F 2005 *Phys. Rev.* B **72** 24449
[10] Spanu L and Parola A 2006 *Phys. Rev.* B **73** 944427
Lante V and Parola A 2006 *Phys. Rev.* B **73** 94427
[11] Darradi R, Richter J and Farnell D J J 2005 *Phys. Rev.* B **72** 104425
[12] Darradi R, Derzhko O, Zinke R, Schulenburg J, Krüger S E and Richter J 2008 *Phys. Rev.* B **78** 214415
[13] Bishop R F, Li P H Y, Darradi R, Schulenburg J and Richter J 2008 *Phys. Rev.* B **78** 054412
See also, Darradi R, Richter J, Schulenburg J, Bishop R F and Li P H Y 2009 *J. Phys.: Conf. Ser.* **145** 012049
[14] Bishop R F, Li P H Y, Darradi R, Schulenburg J, Richter J and Campbell C E 2008 *J. Phys.: Condens. Matter* **20** 415213
[15] Isaev L, Ortiz G and Dukelsky J 2009 *Phys. Rev.* B **79** 024409
[16] Viana J R and de Sousa J R 2007 *Phys. Rev.* B **75** 052403
[17] Carretta P, Melzi R, Papinutto N and Millet P 2002 *Phys. Rev. Lett.* **88** 04701
Melzi R, Carretta P, Lascialfari A, Mambrini M, Troyer M, Millet P and Mila F 2000 *Phys. Rev. Lett.* **85** 1318
Melzi R, Carretta P, Lascialfari A, Mambrini M, Troyer M, Millet P and Mila F 2001 *Phys. Rev.* B **64** 024409
[18] Rosner H, Singh R R P, Zheng W H, Oitmaa J, Drechsler S-L and Pickett W E 2002 *Phys. Rev. Lett.* **88** 186405
Rosner H, Singh R R P, Zheng W H, Oitmaa J, Drechsler S-L and Pickett W E 2003 *Phys. Rev.* B **67** 014416

[19] Capriotti L *et al* 2001 *Phys. Rev. Lett.* **87** 097201
[20] Capriotti L and Sorella S 2000 *Phys. Rev. Lett.* **84** 3173
[21] Takano K, Kito Y, Ono Y and Sano K 2003 *Phys. Rev. Lett.* **91** 197202
[22] du Croo de Jongh M S L L *et al* 2000 *Phys. Rev.* B **62** 14844
[23] dos Anjos R A, Viana J R, de Sousa J R and Plascak J A 2007 *Phys. Rev.* E **76** 022103
See also, Kalz A, Honecker A, Fuchs S and Pruschke T 2008 *J. Phys.: Conf. Ser.* **145** 012051
[24] Okamoto K and Nomura K 1992 *Phys. Lett.* A **169** 433
Nomura K and Okamoto K 1994 *J. Phys. A: Math. Gen.* **27** 5773
[25] Canals B and Lacroix C 1998 *Phys. Rev. Lett.* **80** 2933
[26] Schmidt R, Schulenburg J, Richter J and Betts D D 2002 *Phys. Rev.* B **66** 224406
Oitmaa J and Weihong Z 2004 *Phys. Rev.* B **69** 064416
Majumdar K and Datta T 2009 *J. Phys.: Condens. Matter* **21** 406004
[27] Viana J R, de Sousa J R and Continentino M A 2008 *Phys. Rev.* B **77** 172412
[28] Pavarini E, Tarantino S C, Ballaran T B, Zema M, Ghigna P and Carretta P 2008 *Phys. Rev.* B **77** 014425
[29] Schmalfuß S, Darradi R, Richter J, Schulenburg J and Ihle D 2006 *Phys. Rev. Lett.* **97** 1572011
[30] Filho E B and de Sousa J R 2004 *Phys. Lett.* A **323** 9
Neto J C and de Sousa J R 2005 *Phys. Lett.* A **336** 274
Neto M A and de Sousa J R 2004 *Phys. Rev.* B **70** 224436
[31] dos Anjos R A, Viana J R, de Sousa J R and Plascak J A 2007 *Phys. Rev.* E **76** 022103
[32] Salmon O R, de Sousa J R and Nobre F D 2009 *Phys. Lett.* A **373** 2525